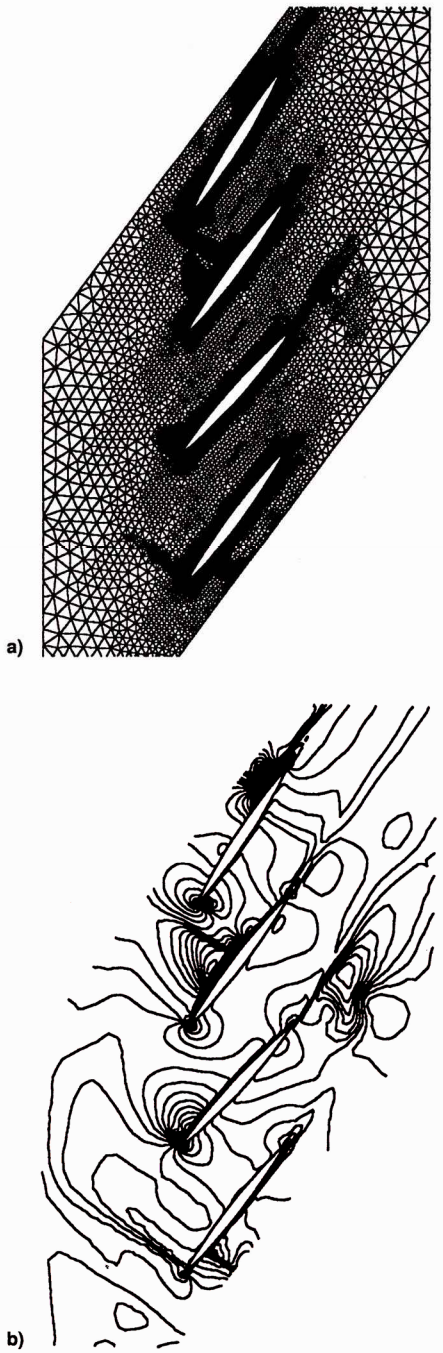

Fig. 3 a) Instantaneous mesh and b) Mach number contour for an oscillating cascade of four blades (k = 0.462, α_0 = 7 deg, α_I = 4.8 deg, σ = 90 deg, and $2Mk\tau = 12\pi$).

are plotted in Fig. 3. From the results given in Fig. 3, shocks appear on the front part of the upper surface of the second blade, and on the midchord of the upper surface of the third blade. Meanwhile, a compression wave on the upper leading edge of the lowest blade is observed. Within the passage between the lowest and highest blades, a shock is depicted that is strong enough to choke the flowfield.

Conclusions

In the present work, a solution-adaptive approach has been presented to investigate the transonic oscillating cascade flows. In a Cartesian coordinate system, the unsteady Euler equations are solved. Comparing the distributions of magnitude and phase angle of the first harmonic dynamic pressure difference coefficient, the present adaptive solutions show better agreement with the experimental data than those from the nonadaptive approach. From the comparison and discussion of instantaneous mesh and Mach number, it is evident that the present adaptive mesh clearly captures the unsteady wave behavior.

References

[1]Wolff, J. M., and Fleeter, S., "Single-Passage Euler Analysis of Oscillating Cascade Aerodynamics for Arbitrary Interblade Phase," *Journal of Propulsion and Power*, Vol. 10, No. 5, 1994, pp. 690–697.

[2]Hwang, C. J., and Yang, S. Y., "Inviscid Analysis of Transonic Oscillating Cascade Flows Using a Dynamic Mesh Algorithm," *Journal of Propulsion and Power*, Vol. 11, No. 3, 1995, pp. 433–440.

[3]He, L., "Unsteady Flow in Oscillating Turbine Cascade Part 2. Computational Study," American Society of Mechanical Engineers, Paper 96-GT-375, June 1996.

[4]Wolff, J. M., and Fleeter, S., "Nonlinear Separated Inviscid-Viscous Analysis of Oscillating Cascade Aerodynamics Using an Inverse Integral Method," American Society of Mechanical Engineers, Paper 97-GT-85, June 1997.

[5]Hwang, C. J., and Fang, J. M., "Solution-Adaptive Approach for Unsteady Flow Calculations on Quadrilateral-Triangular Meshes," *AIAA Journal*, Vol. 34, No. 4, 1996, pp. 851–853.

[6]Buffum, D. H., and Fleeter, S., "The Aerodynamics of an Oscillating Cascade in a Compressible Flowfield," *Journal of Turbomachinery*, Vol. 112, No. 4, 1990, pp. 759–767.

Theoretical Prediction of Mean Droplet Size of Y-Jet Atomizers

H. S. Couto,* J. A. Carvalho Jr.,† and D. Bastos-Netto‡
National Space Research Institute
12630-000 Cachoeira Paulista, Brazil
M. Q. McQuay§
Brigham Young University, Provo, Utah 84602
and
P. T. Lacava¶
National Space Research Institute
12630-000 Cachoeira Paulista, Brazil

Nomenclature

C_d	= discharge coefficient, nondimensional
D_0	= mixing chamber diameter, m
d_l	= ligament diameter, m
f	= constant, nondimensional
h_0	= liquid sheet thickness at the nozzle tip, m
K	= nozzle parameter, defined in Eq. (5), ms
l_0	= mixing chamber length, m
m_{air}	= atomizing airflow rate, kg s^{-1}
m_f	= mass flow rate of liquid, kg s^{-1}
P_c	= chamber pressure, Pa
P_s	= ambient pressure, Pa
P_0	= stagnation pressure, Pa

Received Feb. 21, 1998; revision received Dec. 30, 1998; accepted for publication Dec. 31, 1998.

*Visiting Researcher.
†Senior Researcher.
‡Senior Researcher. Associate Fellow AIAA.
§Professor, Mechanical Engineering Department, 242 CB.
¶Assistant Researcher.

SMD = Sauter mean diameter, m
T_c = chamber temperature, °C
T_0 = stagnation temperature, °C
U_f = liquid sheet velocity, m s^{-1}
U_i = mean value of velocity field, m s^{-1}
U_{1a} = air velocity on one side of the liquid sheet, m s^{-1}
U_{2a} = air velocity on other side of the liquid sheet m s^{-1}
W = Weber number, nondimensional
ΔP_{air} = air pressure drop along the mixing chamber, Pa
ΔP_l = liquid pressure drop along the mixing chamber, Pa
θ = cone semiangle, deg
μ_l = liquid viscosity, kg m^{-1} s^{-1}
ρ_{air} = environment air density, kg m^{-3}
ρ_l = liquid density, kg m^{-3}
σ = liquid surface tension, kg s^{-2}

Introduction

INTERNAL-MIXING, twin-fluid, airblast (Y-jet) atomizers, in which liquid is injected into a mixing chamber with compressed air or steam, are extensively used in industry. Mullinger and Chigier[1] described the operating principles and design guidelines of this type of atomizer in an experimental paper by use of an empirical correlation derived by Wigg[2] to evaluate the effects of flow parameters on the spray droplet mean diameter.

Lefebvre[3] described Wigg's empirical investigation as one that encompassed not only his experimental data, but also those of many other researchers. It did much to elucidate key factors involved in airblast atomization processes and identified the effect of the air velocity on mean droplet size. However, the effects of air density, liquid surface tension, and atomizer size were not clearly established. In particular, Wigg's equation does not offer a good correlation for water sprays. His own explanation for this fact was based on the recombination and/or coalescence of droplets in the spray.

In several types of atomizers, as discussed by Dombrowski and Johns,[4] the liquid is ejected from the final discharge orifice in the form of a thin sheet. The manner in which this sheet is disintegrated in droplets depends on the operating conditions of the nozzle. Squire[5] and Hagerty and Shea[6] analyzed the characteristics of these waves for sheets of inviscid liquids of uniform thickness. Their results were applied with success by Fraser et al.[7] and Dombrowski and Hooper[8] to calculate droplet sizes produced by fan-spray-type injectors working with low-viscosity liquids.

In the model developed by Dombrowski and Johns,[4] the liquid possesses finite viscosity, and the sheet thickness decreases as the distance from the discharge orifice increases. They derived an equation for the average droplet size based on the concept of a planar liquid sheet, and their theoretical values compared well with experimental results obtained by other researchers.

Couto and Bastos-Netto[9] and Couto et al.[10] extended the model of Dombrowski and Johns to sprays formed by two impinging liquid jets, and calculated the corresponding droplet distribution function. With two impinging jets, the liquid sheet remains planar. Their results checked well with the data taken by Queiroz.[11]

The model of Dombrowski and Johns[4] was extended by Couto et al.[12] for pressure-swirl atomizers, for which results checked well with several existing empirical and semi-empirical correlations and experimental data found in the literature. It was assumed that the conical sheet formed by the pressure-swirl atomizer final discharge orifice had, at the time of breakup, a much larger radius than the sheet thickness, and that the wavelength of the ripples formed in the liquid film grew until their amplitude was equal to the ligament radius, so that one droplet is produced per wavelength.[4]

An expression for estimating the film thickness of a Y-jet atomizer is derived in the work reported here, assuming that 1) there is a conical geomery and 2) apart from a small amount of droplets formed by the impact of the liquid on the airstream inside the premixing chamber, the majority of droplets is generated by the liquid film formed inside the premixing chamber wall through the deflection of the liquid jet by the high-speed gas stream flowing along the center core of the chamber. This is to say that the Y-jet atomizer, usually classified as an internal mixing airblast atomizer, behaves instead as a prefilming airblast atomizer. Sauter mean diameter (SMD) values predicted with the formulation developed here compared well with experimental results obtained in a Y-jet atomizer by use of a laser-based, phase Doppler particle analyzer (PDPA).

Problem Description

In a typical Y-jet airblast atomizer, the liquid, on entering the mixing chamber, is pushed against the wall by the incoming pressurized atomizing gas and a liquid film is generated. This liquid film is then ejected from the discharge orifice nearly as a conical sheet that disintegrates into fragments, forming unstable ligaments. These ligaments finally contract under the action of surface tension, and form droplets. Once the film thickness is estimated, the SMD of these droplets is calculated using an analogy based on the work of Dombrowski and Johns,[4] regarding the behavior of a planar disintegrating liquid sheet. They derived an equation for the droplet size based on the concept of a planar liquid sheet, and their theoretical predictions compared well with experimental results. In the present work, the previously mentioned analyses were applied to a Y-jet atomizer in the calculation of atomization parameters for a conical liquid sheet instead of a planar liquid sheet. These parameters include the liquid mass flow rate expression and the liquid film thickness given, as explained next.

Governing Equations

As the atomizing gas and the liquid are discharged together in the surrounding medium, the main parameter in this process is the difference between the chamber pressure P_c and the ambient pressure P_s, which is the same for both fluids, i.e.,

$$\Delta P_l = \Delta P_{\text{air}} = P_c - P_s \tag{1}$$

The liquid sheet velocity is given by

$$U_0 = [C_d(2\Delta P_l/\rho_l)]^{\frac{1}{2}} \tag{2}$$

where the relationship between the film velocity and liquid sheet velocity is $U_f = U_0/\cos\theta$. The continuity equation for incompressible fluids using a conical geometry for the liquid sheet yields

$$m_f = \rho_l U_0(\pi/4)\left[D_0^2 - (D_0 - 2h_0)^2\right] \tag{3}$$

Then from Eq. (3) one has

$$h_0 = \left\{D_0 - \left[D_0^2 - (4m_f/\pi\rho_l U_0)\right]^{\frac{1}{2}}\right\}\Big/2 \tag{4}$$

Dombrowski and Johns[4] derived the following expression for estimating d_l, formed on the liquid film breakup:

$$d_l = 2\left(\frac{4}{3f}\right)^{\frac{1}{3}}\left(\frac{K^2\sigma^2}{\rho_{\text{air}}\rho_l U_i^2}\right)^{\frac{1}{6}}\left(1 + 2.6\mu_l\sqrt[3]{\frac{K\rho_{\text{air}}^4 U_i^8}{6f\rho_l^2\sigma^5}}\right)^{\frac{1}{5}} \tag{5}$$

where K is the "nozzle parameter" that the authors calculated for fan-spray atomizers, and U_i is a velocity term which, for the general case, can be seen to be composed of three components: two of them relative to the air flowing on both sides of the liquid sheet, and the third one relative to the velocity of the sheet itself,[13] U_f. According to Dombrowski and Hooper,[8] $f = 12$ for $W \gg 1$, for either dilational or sinuous breakup. Thus, one obtains from Eq. (5) that

$$d_l = 0.9614\left(\frac{K^2\sigma^2}{\rho_{\text{air}}\rho_l U_i^2}\right)^{\frac{1}{6}}\left(1 + 2.6\mu_l\sqrt[3]{\frac{K\rho_{\text{air}}^4 U_i^8}{72\rho_l^2\sigma^5}}\right)^{\frac{1}{5}} \quad (6)$$

Aside from the variables in Eq. (6), for which expressions have already been obtained, formulations for the velocity profile at the nozzle exit and the nozzle parameter are still missing. For the velocity term U_i, a mean value was chosen such that

$$U_i = \left\{\tfrac{1}{3}\left[U_f^2 + (U_{1a} - U_f)^2 + (U_{2a} - U_f)^2\right]\right\}^{\frac{1}{2}} \quad (7)$$

where U_{1a} and U_{2a} are the air velocities on either side of the sheet. This assumption for U_i is more precise than the one used by Dombrowski and Johns,[4] who simply took an average between velocities on both sides of the sheet. As the ambient air velocity outside the liquid sheet is taken to be zero in the Y-jet atomizer, one may write

$$U_i = \left\{\tfrac{1}{3}\left[2U_f^2 + (U_{1a} - U_f)^2\right]\right\}^{\frac{1}{2}} \quad (8)$$

In this paper, a conical sheet is assumed to be formed from the atomizer final discharge orifice and to possess a much larger radius at the point of rupture than the sheet thickness. Assuming, in addition, that the wavelength of the ripples formed in the liquid film grows until they have an amplitude equal to the radius of the ligament, then one droplet will be produced per wavelength.[4] Once the conical sheet is established, the amplitude of the ripples away from the injector is assumed to be much smaller than the cone diameter, so that disturbances "view" the conical sheet as a plane. With these assumptions, it is possible to apply the theory developed for thin planar liquid sheets to thin conical liquid sheets.

A relationship is needed relating the location along the liquid sheet to the local sheet thickness, which eventually will be related to the initial thickness of the sheet at the nozzle tip (known quantity). At any location, by conservation of mass, as the position along the liquid sheet increases, the thickness of the sheet decreases. For a planar sheet, the thickness at any section X (X being the position measured from the nozzle tip to the rupture point) was described by Dombrowski and Johns[4] as a function of the local sheet thickness h, as $h = K_1/X$, where K_1 is a constant. In the present work, as the liquid sheet radiates as a conical sheet from the nozzle tip with uniform velocity, the thickness at any section is also considered to be given by $h = K_1/X$. Dombrowski and Johns, assuming a hyperbolic relationship between the local sheet thickness h and time t, used $K = ht$, where K is the nozzle parameter introduced in Eq. (5). Therefore,

$$K = K_1 t/X = K_1/U \quad (9)$$

The only way for the condition in Eq. (9) to hold true is that at a coordinate $X = nh_i$, where n is any positive number and h_i is the initial sheet thickness at the atomizer tip where the conical liquid surface is formed. Therefore, the sheet thickness will be given by h_i/n. Thus,

$$K_1 = (h_i/n)nh_i = h_i^2 \quad (10)$$

$$K = h_i^2/U_f \quad (11)$$

As discussed by Wang and Lefebvre,[14] $h_i = h_0\cos\theta$, and for incompressible flow, $U_f = U_0/\cos\theta$, where U_0 is the liquid velocity at the atomizer tip. Consequently,

$$K = \frac{h_0^2\cos^3\theta}{U_0} \quad (12)$$

Inserting Eq. (12) into the equation derived by Dombrowski and Johns[4] for the ligament diameter in a planar sheet [Eq. (6)], the following equation is obtained for a conical sheet, where U_i is given by Eq. (8):

$$d_l = 0.9614\left(\frac{h_0^4\sigma^2\cos^6\theta}{\rho_{\text{air}}\rho_l U_f^2 U_i^2}\right)^{\frac{1}{6}}\left(1 + 2.6\mu_l\sqrt[3]{\frac{h_0^2\rho_{\text{air}}^4 U_i^8\cos^3\theta}{72U_f\rho_l^2\sigma^5}}\right)^{\frac{1}{5}} \quad (13)$$

for the diameter of the ligaments, which, according to Rayleigh (in Lefebvre[15]) will generate droplets with

$$\text{SMD} = 1.89d_l \quad (14)$$

The discharge coefficient was estimated as[16]

$$C_d = 0.827 - 0.008l_0/D_0 \quad (15)$$

where l_0 is the mixing chamber length taken from the liquid injection point. The spray angle was estimated by the relation given by Abramovich[17]:

$$\tan\theta = 0.13[1 + (\rho_{\text{air}}/\rho_l)] \quad (16)$$

This angle can, alternatively, be measured directly by photographic methods.

Experimental Setup and Procedure

To validate the mathematical development proposed here, a Y-jet atomizer was built and SMD measurements were carried out with a two-component, laser-based, PDPA system. A schematic of the Y-type atomizer used in this work is shown in Fig. 1. The atomizer dimensions, basically the liquid and air-injection orifices and the mixing chamber dimensions, were calculated using Mullinger and Chigier's guidelines[1] and the following assumptions: 1) isentropic flow through the atomization air orifice, 2) Mach number equal to unity at the air orifice outlet section, 3) stagnation air temperature of 298 K, and 4) liquid injection discharge coefficient of 0.75. At the design operating conditions, the ratio between the atomization air to the liquid flow rates was chosen to be 0.1.

Experiments with water were performed for atomization air-injection pressures of 8, 15, and 25 psig. In these tests, the air mass flow rate was measured with a calibrated orifice plate and the water mass flow rate with a rotameter. The following parameters were then calculated, under the assumption of isentropic flow through the air-injection orifice: injection Mach number, air density, stagnation pressure, and temperature in the mixing chamber. The air velocity at the end of the mixing chamber was calculated from the chamber dimensions, using the calculated air density, and the ratio between the air and liquid mass flow rates. For characterization with the PDPA system, the atomizer was positioned in the vertical direction with its tip pointed downward and the laser beams in

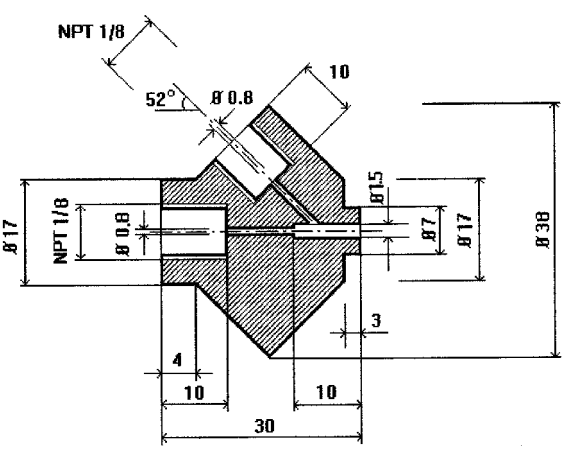

Fig. 1 Y-jet atomizer tested in this work (dimensions in millimeters).

the horizontal direction. Measurements presented here were taken at the spray centerline at an axial position of 7.6 cm below the nozzle tip.

Comparison of Theoretical and Experimental Results

Table 1 presents the variation of several atomizer flow parameters as the water mass flow rate was varied, for air stagnation pressures of 8, 15, and 25 psig, respectively. The parameters shown in Table 1 are important here because they are the parameters used in the evaluation of all the variables needed in the proposed mathematical formulation.

Figure 2 shows the variation of the SMD with water mass flow rate for atomizing air injection pressures of 8, 15, and 25 psig. The SMD was obtained for the following cases: 1) by use of the formulation developed in this paper and 2) by experimental determination with the PDPA system. The nozzle-operating conditions were not extended to water mass flow rates above 5 g/s because, in this case, the SMD values obtained would be comparable with the PDPA measurement volume, leading to nonreliable experimental results.

As shown in Fig. 2, as the liquid mass flow rate increases, the SMD increases. SMD also increases for a given liquid mass flow rate as the nozzle operating pressure increases. It is observed that the results obtained with the theoretical formulation derived in this work fit the experimental data well. One of the strong features of the formulation is that it takes into account the atomizer geometrical characteristics through the nozzle parameter K. The SMD has been shown to be very sensitive to K, which in turn, is strongly dependent on the liquid film thickness h_0. Therefore, by measuring the droplet SMD, one may conclude that the expression derived for h_0, i.e.,

Table 1 Atomizer flow parameters for ΔP_l = 8, 15, and 25 psig[a]

P_0, psig	m_f, g/s	m_{air}, g/s	Mach number	T_c/T_0	P_c/P_0	ρ_{air}, 10^3 kg m^{-3}	T_c, °C	ΔP_l, bar	U_i, m/s	SMD calculated, μm	SMD measured, μm
8	2.40	0.112	0.384	0.971	0.903	1.69	19.4	0.50	132	64	64
8	3.60	0.092	0.305	0.982	0.938	1.75	19.6	0.52	105	85	86
8	4.20	0.078	0.255	0.987	0.956	1.77	19.7	0.53	88	95	100
8	5.10	0.073	0.238	0.989	0.961	1.78	19.8	0.53	82	111	104
8	6.30	0.067	0.216	0.998	0.968	1.80	20.0	0.53	74	133	——
15	2.40	0.176	0.485	0.955	0.851	2.10	19.1	0.88	166	47	45
15	3.60	0.146	0.382	0.972	0.904	2.22	19.4	0.93	131	61	56
15	4.20	0.131	0.336	0.978	0.925	2.26	19.6	0.95	115	68	74
15	5.10	0.114	0.287	0.984	0.944	2.30	19.7	0.97	98	77	82
15	6.30	0.105	0.263	0.986	0.953	2.32	19.7	0.98	90	91	86
25	2.40	0.235	0.479	0.956	0.855	2.85	19.1	1.48	164	34	42
25	3.60	0.231	0.469	0.958	0.860	2.86	19.2	1.49	161	47	46
25	4.20	0.216	0.431	0.964	0.880	2.91	19.3	1.52	148	52	54
25	5.10	0.190	0.337	0.978	0.924	3.27	19.6	1.60	116	58	61
25	6.30	0.168	0.319	0.980	0.932	3.05	19.6	1.61	109	68	67

[a] $T_0 = 20°C$, $\theta = 7$ deg, as measured from photographs of the spray.

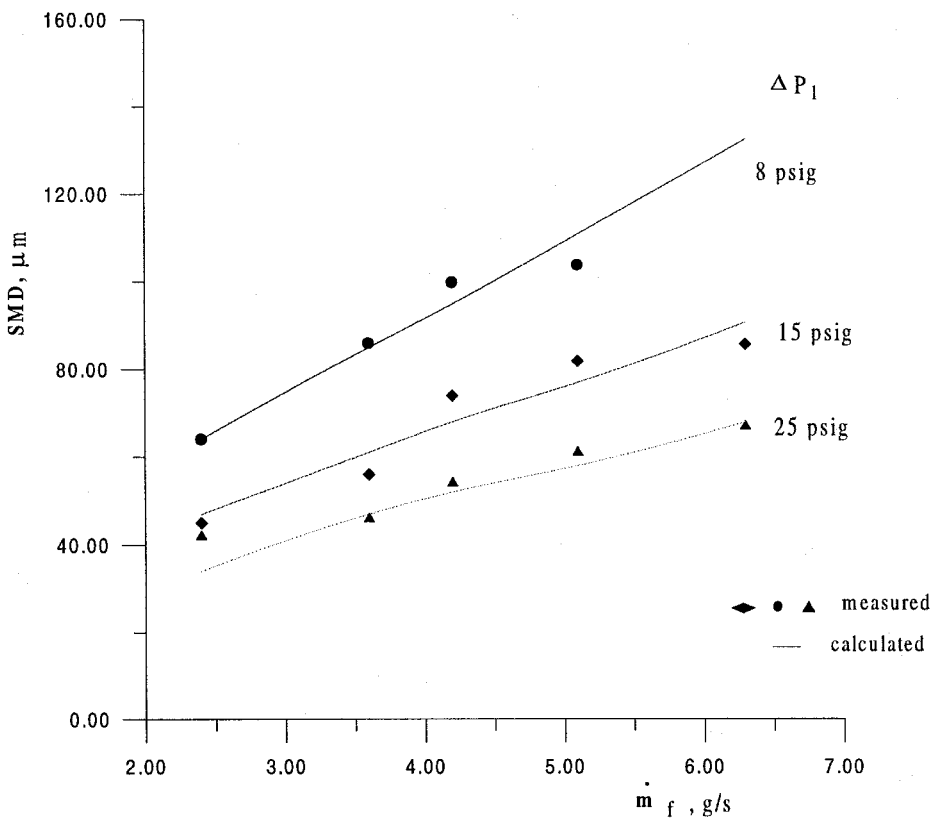

Fig. 2 SMD (calculated and measured) vs water mass flow rate, ΔP_l = 8, 15, and 25 psig.

Eq. (4), is satisfactory in describing the overall phenomenon of the liquid film generation.

Conclusions

A theoretical formula for estimating the SMD, based on Dombrowski and Johns' hypothesis[4] regarding the thickness of a planar disintegrating liquid sheet, was derived for a Y-jet atomizer, considering a conical surface for the disintegrating sheet. The derived theoretical equation for the conical spray SMD atomizer includes geometrical parameters as well as easy-to-measure liquid fuel and atomizing gas flow parameters; and it correlates satisfactorily with experimental data obtained with water.

The only formulation available to date for estimating the SMD of Y-jet atomizers was that given by Wigg's equation.[2] It does not perform well for water. The present formulation has been shown to work for water, not only for Y-jet atomizers, but also for pressure swirl atomizers.[12] For pressure swirl atomizers, using experimental results from other sources, the formulation has been shown to perform reasonably for other liquids, such as diesel fuel, heavy fuel oil, ethyl alcohol, and kerosene. The formulation developed here can be applied for $W \gg 1$, which was the case in all of the experimental data presented, for which $33 < W < 161$.

Acknowledgments

The authors are grateful for FAPESP, Research Support Foundation of the State of São Paulo, Brazil, Project 95/0455-8, for the financial support of H. S. Couto as a Visiting Professor at the Instituto Nacional de Pesquisas Espacias. The authors are also indebted to the National Science Foundation, Grant INT-9302321; and CNPq, National Research Council, Brazil, Project 910153/92-2, for financial support of this work.

References

[1]Mullinger, P. J., and Chigier, N. A., "The Design and Performance of Internal Mixing Multijet Twin Fluid Atomizers," *Journal of Institute of Fuel*, Vol. 47, No. 393, 1974, pp. 251–261.

[2]Wigg, L. D., "Drop-Size Prediction for Twin-Fluid Atomizers," *Journal of Institute of Fuel*, Vol. 37, No. 286, 1964, pp. 500–505.

[3]Lefebvre, A. H., "Airblast Atomization," *Progress in Energy and Combustion Science*, Vol. 6, No. 3, 1980, pp. 233–261.

[4]Dombrowski, N., and Johns, W. R., "The Aerodynamic Instability and Disintegration of Viscous Liquid Sheets," *Chemical Engineering Science*, Vol. 18, No. 2, 1963, pp. 203–214.

[5]Squire, H. B., "Investigation of the Instability of a Moving Liquid Film," *British Journal of Applied Physics*, Vol. 4, No. 6, 1953, p. 167.

[6]Hagerty, W. W., and Shea, J. F., "A Study of the Stability of Moving Liquid Film," *Journal of Applied Mechanics*, Vol. 22, No. 4, 1955, pp. 509–514.

[7]Fraser, R. P., Eisenklam, P., Dombrowski, N., and Hasson, D., "Drop Formation from Rapidly Moving Liquid Sheets," *AIChE Journal*, Vol. 8, No. 5, 1962, pp. 672–680.

[8]Dombrowski, N., and Hooper, P. C., "The Effect of Ambient Density on Drop Formation in Sprays," *Chemical Engineering Science*, Vol. 17, No. 2, 1962, p. 291.

[9]Couto, H. S., and Bastos-Netto, D., "Modeling Droplet Size Distribution from Impinging Jets," *Journal of Propulsion and Power*, Vol. 7, No. 4, 1991, pp. 654–656.

[10]Couto, H. S., Bastos-Netto, D., and Migueis, C. E., "Modeling of the Initial Droplet Size Distribution Function in the Spray Formed by Impinging Jets," *Journal of Propulsion and Power*, Vol. 8, No. 3, 1992, pp. 725–727.

[11]Queiroz, L. C., "Experimental Determination of the Local Mean Diameter of Droplets Generated by Impinging Jets," M.Sc. Dissertation (in Portuguese), Inst. Nacional de Pesquisas Espacias, Cachoeira Paulista, SP, Brazil, March 1992.

[12]Couto, H. S., Carvalho, J. A., Jr., Bastos-Netto, D., "Theoretical Formulation for Sauter Mean Diameter of Pressure-Swirl Atomizers," *Journal of Propulsion and Power*, Vol. 13, No. 5, 1997, pp. 691–696.

[13]Shen, J., and Li, X., "Breakup of Annular Viscous Liquid Jets in Two Gas Streams," *Journal of Propulsion and Power*, Vol. 12, No. 4, 1996, pp. 752–759.

[14]Wang, X. F., and Lefebvre, A. H., "Mean Drop Sizes from Pressure-Swirl Nozzles," *Journal of Propulsion and Power*, Vol. 3, No. 1, 1987, pp. 11–18.

[15]Lefebvre, A. H., *Atomization and Sprays*, Hemisphere, New York, 1989.

[16]Lichtarowicz, A., Duggins, R. K., and Markland, E., "Discharge Coefficients for Incompressible Non-Cavitating Flow Through Long Orifices," *Journal of Mechanical Engineering Science*, Vol. 7, No. 2, 1965, pp. 210–219.

[17]Abramovich, G. N., *Theory of Turbulent Jets*, MIT Press, Cambridge, MA, 1963.

Optimal Performance of Enthalpy Rocket

Lorenzo Casalino* and Guido Colasurdo†
Turin Politechnic Institute, 10129 Turin, Italy

Introduction

THE theoretical performance of an enthalpy rocket has recently been discussed in several published Notes.[1–3] The rocket uses the stored energy of a thermal capacitor to heat a nonreacting working fluid. Parker and Humble[1] derived the velocity increment of a rocket that only consists of the capacitor and propellant masses. The released energy during the solidification of a suitable material heats the propellant from an absolute zero temperature to the material's melting temperature. Different materials and working gases have been compared; the heavier propellants appeared to hold some promise for applications requiring sizable velocity increments. Gany[2] has shown that the performance of an enthalpy rocket with no payload or additional inerts, other than the capacitor itself, is merely a function of capacitor and propellant thermodynamic properties. King[3] suggests some means to improve engine performance; in particular, he points out the benefit of a higher initial temperature of the working fluid and suggests a more complete use of the capacitor mass by allowing its temperature to range from values above the melting point to temperatures below it. Performance is also improved by heating the propellant to a lower temperature, i.e., by expelling the gas with a lower exhaust velocity but in larger quantities for unit mass of capacitor. King also proposes the use of nitrogen in the early phase of the engine operation and then a subsequent shift to hydrogen.

This Note investigates the theoretical upper limits of the enthalpy rocket by applying the theory of optimal control.[4] The assumptions of perfect heat transfer and negligible heat of vaporization for an initially liquid propellant do not reduce performance and appear to be coherent with the aim of the work. However, the application of the control theory has been directed to analyze the influence of the relevant parameters more than to obtain the ideal engine performance. In particular, this Note addresses the selection criteria for the capacitor material and working fluid, the influence of the propellant temperature inside its tank, and the best choice for the total temperature of the heated propellant, which is not constant during the engine operation.

Previous analyses have assumed that the whole rocket mass is functional, i.e., consisting of capacitor and propellant, to obtain the highest velocity increment; under the same conditions, conventional propulsion provides infinite velocity. The presence of a payload and inert mass apart from that of the capacitor is accounted for in this work and comparisons are more favorable for the enthalpy rocket. The tank mass is related to the physical state of the working fluid, and therefore, to its initial temperature; this aspect has not been considered.

Received Sept. 4, 1998; revision received Nov. 23, 1998; accepted for publication Dec. 5, 1998.

*Researcher, Dipartimento di Energetica, Corso Duca degli Abruzzi, 24. Member AIAA.

†Professor, Dipartimento di Energetica, Corso Duca degli Abruzzi, 24. Senior Member AIAA.